



# An Alternative Optimal Design of Dynamic Straight-Right Lane Control for T-Shaped Intersections

Yin HAN<sup>1</sup>, Bo NING<sup>2</sup>, Shidong LIANG<sup>3</sup>

Original Scientific Paper  
Submitted: 11 Sep. 2023  
Accepted: 4 Jan. 2024

<sup>1</sup> 13166222211@126.com, Business School, University of Shanghai for Science and Technology

<sup>2</sup> fulandiningbo@163.com, Business School, University of Shanghai for Science and Technology

<sup>3</sup> Corresponding author, sdliang@hotmail.com, Business School, University of Shanghai for Science and Technology



This work is licensed under a Creative Commons Attribution 4.0 International License.

Publisher:  
Faculty of Transport and Traffic Sciences,  
University of Zagreb

## ABSTRACT

A novel control method called dynamic straight-right lane (DSRL) control design is proposed for signalised intersections. This design aims to utilise the resources of the right-turn lane to increase the capacity for straight-through traffic while minimising the impact on right-turn vehicles. In this paper, an alternative approach to DSRL control design for T-shaped intersections is proposed. By redesigning the spatial and temporal allocation at the entrance, this design ensures the safety of lane change manoeuvres and reduces the design threshold for T-shaped intersections. To facilitate the implementation of the DSRL control design, a cellular automata model is constructed. Additionally, a case study is conducted, leading to the identification of the optimal design parameters for DSRL control. The proposed DSRL control design is compared with two conventional control designs, namely dedicated right-turn lane control design and static straight-right lane control design, in various geometric and traffic demand scenarios. The findings reveal that the T-shaped intersection, when equipped with a dedicated right-turn lane control design, can achieve a maximum delay optimisation rate of 91% by adopting the DSRL control design. Similarly, the T-shaped intersection, with a static straight-right lane control design, can attain a maximum delay optimisation rate of 84% when employing the DSRL control design.

## KEYWORDS

T-shaped intersections; dynamic control; cellular automata; traffic optimisation.

## 1. INTRODUCTION

### 1.1 Motivation

With the increasing conflict between transportation supply and demand, achieving efficient traffic operation within the limited road space in urban transportation poses a significant challenge. T-shaped intersections serve as crucial transition nodes in urban road traffic, and optimising their spatial and temporal control is vital to ensure the smooth flow of urban roads. Owing to the inadequacy of traditional intersection design and optimisation methods in meeting the rapidly growing traffic demand, many scholars have started exploring unconventional approaches to intersection control design. These unconventional design concepts encompass median U-turns [1, 2], contraflow left-turn lane design [3, 4], variable lane design [5, 6] and more recently, the design of dynamic straight-right lane (DSRL) control [7, 8].

The primary objective of numerous unconventional designs is to mitigate the vehicle queuing phenomenon and, consequently, enhance intersection traffic efficiency. Therefore, many scholars have studied the queuing phenomenon of vehicles at intersections [9–13]. The recently proposed DSRL control design addresses the queuing problem of vehicles, which has been identified as an effective control method for enhancing vehicular traffic efficiency at signalised intersections. In the design of DSRL control, the primary objective is to utilise the resources of the right-turn lane to augment the capacity for straight-through traffic

while minimising the impact on right-turn vehicles. Nevertheless, the existing design of DSRL control encounters challenges in lane changing. To address this issue, this paper proposes a DSRL control design specifically for T-shaped intersections, which integrates the design principles of contraflow left-turn lane control and variable lane control.

## 1.2 Literature review

Numerous studies have been conducted on contraflow left-turn lane control and variable lane control. Therefore, this paper provides a comprehensive review of the research conducted in these two areas.

The contraflow left-turn lane has been identified as an effective method for enhancing the operational efficiency of intersections. This approach increases intersection capacity by dynamically opening exit lanes for left-turn traffic using additional traffic lights known as pre-signals, which are installed at intermediate openings [14]. Another way to improve the capacity of signalised intersections is by incorporating a dedicated left-turn phase [15]. Constructing a cellular automata model to evaluate the best match between the length of the reverse left-turn lane and the duration of the pre-signal green light is also considered a good approach [16]. However, this requires the estimation of the left-turn queue length under the contraflow left-turn lane design [17]. To enhance the operational efficiency of intersections with limited lanes and short vehicle queues, a new design combining tandem control and left-turn control for exit lanes has been proposed [18]. With the advancement of technology, the operational design of contraflow left-turn lane control can be further improved and optimised through the integration of detectors [19]. Scholars have assessed the benefits of contraflow left-turn lane control by studying queuing scenarios and developing analytical models [20, 21]. The effect of upstream intersections on contraflow left-turn design performance has also been analysed and studied [22].

By implementing dynamic reversible lanes, variable lane control has been shown to significantly increase roadway capacity without major changes to the roadway structure, control facilities, or traffic infrastructure [23]. The design of variable lane control involves the combination of traffic signals and variable guide lanes [5] and can be tailored to the specific needs of the road network to improve its rationality [24]. It is also possible to use the field data to dynamically assign lanes to intersections, thereby reducing the saturation flow rate of intersection lanes [25]. A bi-level formulation has been proposed to study the problem of time-varying lane capacity reversibility based on traffic management [26]. Algorithmic control of variable lanes has also been proposed to improve control efficiency [27]. Furthermore, some scholars have improved lane utilisation by dynamically adjusting the lane function and reconfiguring the lane combinations [28, 29]. Variable lane control plays an important role in the evacuation network optimisation problem [30]. Invoking the concept of influence area also enables the benefits of variable lane control to be further improved [31].

## 1.3 Proposed approach and contribution

These studies have made significant contributions to enhancing the efficiency of signalised intersections. Contraflow left-turn lane control focuses on utilising the opposing lane. However, when the opposing lane is limited to one lane, it can hinder the travel of right-turn vehicles at the adjacent entrance. Variable lane control enhances the efficiency of vehicle movement at intersections by adjusting lane functions according to different times of the day. Variable lane control for better optimisation, the function of a specific lane is typically maintained for an extended duration. This necessitates the consideration of alternative control methods to address the requirement for frequent lane function changes.

The DSRL control method proposed in this paper combines the design concepts of contraflow left-turn lane control and variable lane control, enabling effective lane change behaviour and ensuring safe vehicle passage at T-shaped intersections. Moreover, this control method reduces the requirements for intersection capacity, allowing for the utilisation of T-shaped intersections with a limited number of lanes. Pre-signal control is a common feature in various unconventional control methods [32–35]. In this paper, we integrate pre-signals with contraflow left-turn lane control, enabling DSRL control to effectively accommodate frequent lane change operations. The proposed design involves dividing the entrance into three sections:

a straight-through lane (STL), a right-turn lane (RTL) and a DSRL. Pre-signals are utilised to temporally segregate straight-through and right-turn vehicles on the DSRL, facilitating safe lane changes. Furthermore, this method optimises the use of surplus space-time resources in the RTL to mitigate traffic congestion in the STL, resulting in reduced delays at T-shaped intersections. The contributions of this paper can be summarised as follows.

- 1) This paper introduces an alternative DSRL design that aims to reduce average vehicle delay at T-shaped intersections while ensuring safe lane change behaviour. The design achieves these objectives by reconfiguring the entrance space of the intersection. Additionally, this reduces the demand for intersections to implement this control method.
- 2) This paper constructs a simulation model using cellular automata (CA) to simulate the DSRL design. The proposed CA model in this paper incorporates the design ideas of DSRL into the NS model [36], thus providing a simulation model and a comprehensive database for future research.
- 3) This paper proposes an optimisation model to determine the design parameters of DSRL. The optimisation model considers the traffic conditions at the entrance of the T-shaped intersection and identifies the optimal solution for DSRL design parameters. This approach maximises the utilisation of spatial and temporal resources at the entrance, enhancing the efficiency of DSRL control design.

#### 1.4 Research steps

In the following sections, Section 2 will provide a brief description of the DSRL design concept. Section 3 will focus on the construction of a simulation model of CA and an optimisation model of design parameters for DSRL. Section 4 will use a case study to determine the optimal design parameters for DSRL and compare the effects of two conventional control designs with the optimal DSRL control design effects. Finally, the last section will conclude the paper and offer insights into future research directions.

## 2. DESIGN CONCEPT

The DSRL design proposed in this paper focuses on redistributing the space-time resources at the entrance of T-shaped intersections. At each entrance of the T-shaped intersection, two traffic flows exist, without taking vehicle turnaround into account. Assume that this limited-lane T-shaped intersection has only two lanes at the entrance. To facilitate the study, one entrance is selected, and it consists of two lanes: the straight-through lane and the straight-right lane. At the entry point, the straight-through traffic and the right-turn traffic are separated and do not affect each other.

### 2.1 Traffic lane layout design

The entrance is divided into three sections, an STL, an RTL and a DSRL. Each lane is equipped with a signal that controls the flow direction and traffic status, as illustrated in *Figure 1*. Signal S1, located in the STL, serves as the primary signal of the intersection, controlling the traffic flow. As a result, signal S1 also regulates the traffic flow in the STL. The end of the DSRL creates an opening towards the STL, allowing straight-through traffic to enter the DSRL. Signal S2 is placed at the opening of the DSRL to regulate the

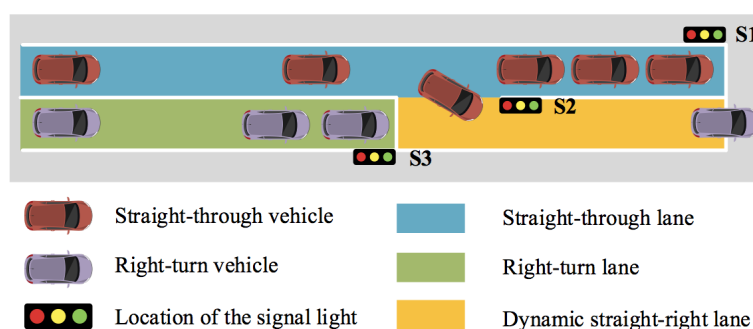


Figure 1 – Traffic lane layout design for dynamic straight-right lanes

priority of entry for straight-through vehicles into the DSRL. Signal S3, positioned at the stop line of the RTL, determines the right-of-way for right-turn vehicles entering the DSRL.

**2.2 Traffic control strategy at the intersection**

DSRL control design aims to ensure vehicle safety while maximising the utilisation of intersection time. In this paper, the timing scheme of the signal group at the entrance is designed for improvement based on the timing scheme of the intersection's main signal. Each signal has a distinct operation scheme, and the combination of these three signals forms a signal group, as depicted in Table 1 and Figure 2.

Table 1 – Rules for the moving of vehicles

	Straight-through lane	Right-turn lane	Dynamic straight-right lane	
	Straight-through vehicles	Right-turn vehicles	Straight-through vehicles	Right-turn vehicles
Phase 1	queue	move	×	√
Phase 2	queue	queue	√	×
Phase 3	move	queue	√	×
Phase 4	move	move	×	√

Note: "√" means access is permitted, "×" means access is prohibited.

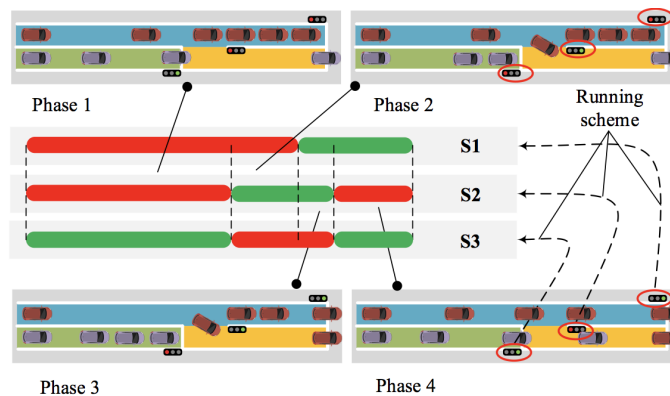


Figure 2 – Traffic control strategy at the intersection for dynamic straight right lanes

In phase 1, the main signal S1 displays a red light, causing vehicles to queue in STL. Signal S2 also displays a red light, preventing vehicles from accessing DSRL. Meanwhile, signal S3 shows a green light, granting right-turn vehicles the right-of-way to use DSRL. The main signal does not regulate right-turn vehicles entering DSRL and can pass through the intersection without any restrictions.

In phase 2, the main signal S1 remains red, causing already queued vehicles in STL to continue waiting for the signal to turn green. Signal S2 displays a green light, allowing vehicles to use DSRL. On the other hand, signal S3 shows a red light, prohibiting right-turn vehicles from entering the DSRL.

In phase 3, the main signal S1 turns green, granting permission for the queued-through vehicles in STL and those entering DSRL to cross the intersection. Signal S2 remains green, allowing continuous usage of DSRL through vehicles. However, signal S3 remains red, maintaining the prohibition on right-turn vehicles from entering the DSRL.

In phase 4, the main signal S1 turns green, allowing all vehicles to proceed. Signal S2 turns red, prohibiting through vehicles from entering the DSRL. Vehicles that have not entered the DSRL lane should use the STL for travel. Meanwhile, signal S3 returns to green, permitting right-turn vehicles to utilise DSRL once again.

**3. MICRO-SIMULATION BASED ON CELLULAR AUTOMATA**

The CA model is favoured by many scholars [37–41] for traffic simulation due to its simple rules and high efficiency.

### 3.1 Model parameters and variables

To facilitate the model representation, Table 2 summarises the key notations of model parameters and variables used in this paper.

Table 2 – Basic parameter table

Parameters and variables	Meanings
$T$	Cycle time of signal group timing scheme (s)
$t_r$	Length of red light for main signal S1 (s)
$t_i$	Without delay passage time for vehicle $i$ (s)
$t_s^{S2}$	The moment of signal S2 turns on the green light (s)
$t_f^{S2}$	The moment of signal S2 ends green (s)
$L$	Length of dynamic straight-right lane (m)
$L_o$	Length at opening (m)
$L_1$	Length of the simulation environment (m)
$x_i$	Location of $i$ car
$N$	Number of operating vehicles
$N_d$	The lane parking capacity of the dynamic straight right lane
$n_t$	Number of periods in the whole day
$Q$	Practical capacity of one lane (veh/h)
$v_f$	Free-flow speed of vehicle (km/h)
$k_j$	Jam density (veh/km)

### 3.2 Operating environment

To construct the operating environment for the CA model, one of the entrances of the T-shaped intersections is selected as the focus of the study. The simulation was conducted in the operating area of the intersection entrance, which extends from the parking line to  $L_1$  upstream of the entrance. Figure 3 demonstrates the treatment of the operating area based on the design principles of DSRL control, including the provision of an opening area for the movement of straight-through vehicles into the DSRL.

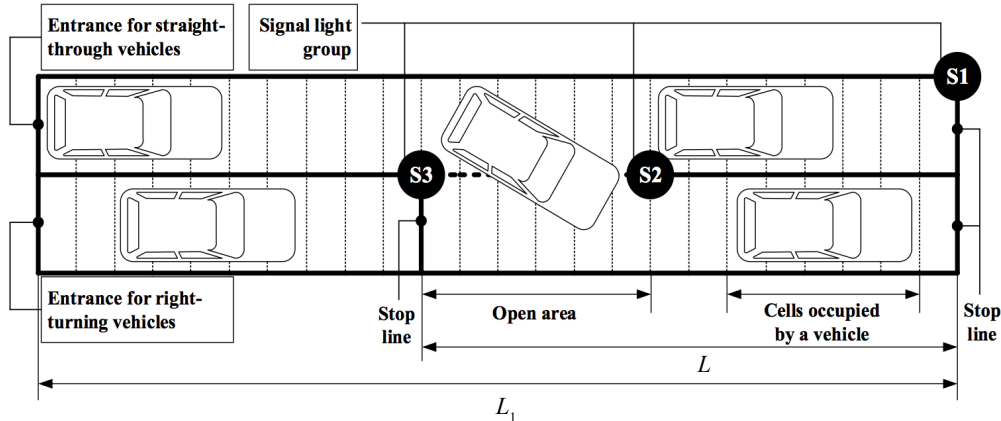


Figure 3 – Cellular automata for the design of dynamic straight-right lane control

The entrance of vehicles serves as the starting boundary for the operating environment, with  $x_i=0$  indicating that the vehicle has entered the operating environment. The stop line at the main signal S1 is designated as the termination boundary of the operating environment. When the vehicle position exceeds  $x_i>L_1$ , the vehicle exits the operating environment.

### 3.3 Operating rules

NS model [36] is widely used in the traffic flow model of CA. In this paper, based on the NS model, we add the DSRL design content to construct the CA model.

Signals S1 and S2 regulate the movement of straight-through vehicles. The simulation time,  $t_m$ , is governed by Equation 1, which determines when signal S1 is released for straight-through vehicles. Similarly, Equation 2 governs the simulation time for signal S2, enabling the entry of straight-through vehicles into the DSRL. To ensure the safety of straight-through vehicles entering the DSRL, right-turn vehicles are required to come to a stop and wait. Signal S3 is responsible for controlling the right-turn vehicles, and when Equation 2 is satisfied, it prohibits right-turn vehicles from proceeding.

$$t_r \leq \text{mod}(t_m, T) \leq T \tag{1}$$

$$t_s^{S2} \leq \text{mod}(t_m, T) \leq t_f^{S2} \tag{2}$$

where  $\text{mod}(a,b)$  is the remainder function, which calculates the remainder of  $a/b$ .

Straight-through vehicles are permitted to change lanes only at the opening when signal S2 is green. The opening area has a length of  $L_o$ , and for straight-through vehicles to execute a lane change during green signal S2, their position must satisfy Equation 3.

$$L_1 - L \leq x_i(L_1 - L) + L_o \tag{3}$$

The safe distance refers to the distance between the vehicle entering the DSRL and the last vehicle in the DSRL. The headway of vehicles in congested traffic is set to the minimum safe distance. If the headway between the vehicle entering the DSRL and the last vehicle in the DSRL satisfies Equation 4, the vehicle is allowed to enter the DSRL and proceed.

$$x_i \leq x_d^j - 1000/k_j \tag{4}$$

where  $x_d^j$  is the position of the last car in DSRL.

#### 4. OPTIMISATION MODEL OF THE DYNAMIC STRAIGHT-RIGHT LANE

The lane-parking capacity of the DSRL and the moment of signal S2 on the green are important factors that affect the design efficiency of the DSRL control. Assume that the vehicle arrivals follow Poisson distribution and that the straight-through vehicles have been segregated from the right-turn vehicles at the entrance. To achieve the optimal control effect, this paper will develop an optimisation model to optimise the lane-parking capacity of the DSRL and the timing of signal S2 turning green.

##### 4.1 Optimisation objectives

The arrival time of a vehicle at the entrance is denoted as  $t_{ca}^i$ . The departure time of the vehicle from the entrance is denoted as  $t_{cl}^i$ . The difference in the lane-parking capacity of DSRL and the start-up moment for the green light of signal S2 affects the time for vehicles to leave the entrance. Take  $t_{cl,L,t_s^{S2}}^i$  as the moment for vehicles to leave the entrance with different design parameters. In this paper, the optimisation objective is to minimise the average delay of vehicles. The lane-parking capacity of the DSRL and the timing of signal S2 turning on the green light are considered variables in the optimisation to determine the optimal parameters for the design of T-shaped intersections, as shown in Equation 5.

$$f(N_d, t_s^{S2}) = \min_{N_d, t_s^{S2}} \left\{ \frac{\sum_{i=1}^N [(t_{cl,L,t_s^{S2}}^i - t_{ca}^i) - t_i]}{N} \right\} \tag{5}$$

The optimal design parameters for DSRL control are influenced by varying traffic flow arrival conditions. The optimal parameters for DSRL control design fluctuate throughout the day due to varying traffic operations at the intersection. In practice, it is relatively challenging to regulate both the lane-parking capacity of the DSRL and the timing of the green signal activation for S2. Therefore, this paper focuses on optimising the lane-parking capacity of the DSRL. The entire day is divided into  $n_t$  time periods, and the DSRL of lane-parking capacity is treated as the independent variable to determine the minimum average vehicle delay using Equation 5 for each time period. And calculate the total vehicle delay in each time period as  $g_k = f_k(N_d, t_s^{S2}) \cdot N_k$ , where  $f_k(N_d, t_s^{S2})$  is the average vehicle delay under the optimal design parameters of DSRL

control for time period  $k$ .  $N_k$  is the total number of vehicles in time period  $k$ . The total vehicle delays are calculated for different capacities for the whole day. The DSRL of lane-parking capacity that results in the lowest total delay is considered the optimal lane-parking capacity, as indicated by Equation 6.

$$h(L) = \min_L \sum_{k=1}^{n_t} g_k \tag{6}$$

The optimal DSRL of lane-parking capacity is determined for the target entrance, and the timing of signal S2 turning on the green light is adjusted based on the traffic volume at different times using Equation 5.

### 4.2 Constraints

If the length  $L$  of DSRL is too short, it will have an impact on the design function. The length  $L$  of DSRL is correlated with its lane-parking capacity, so it is necessary to design the minimum lane-parking capacity  $\min N_d$  vehicles and the maximum lane-parking capacity  $\max N_d$  vehicles for DSRL. The constraint on the length  $L$  of DSRL can be expressed by Equation 7, which is based on the jamming density  $k_j$  at the target entrance.

$$\min N_d \cdot \frac{1000}{k_j} \leq L \leq \max N_d \cdot \frac{1000}{k_j} \tag{7}$$

The timing scheme of the signal group starts at the moment when the main signal S1 turns on the red light. In Figure 4, signal S1 turns on the red light at the beginning of the cycle (0<sup>th</sup> second), followed by the green light after  $t_r$  seconds. The green light period lasts for  $T-t_r$  seconds, and then a new cycle begins. For signal S2, the green light period starts at the beginning of the cycle after  $t_s^{S2}$  seconds, and it ends after  $t_f^{S2}$  seconds. The rest of the cycle is red. Signal S3 is green when signal S2 is red, and it turns red when signal S2 is green.

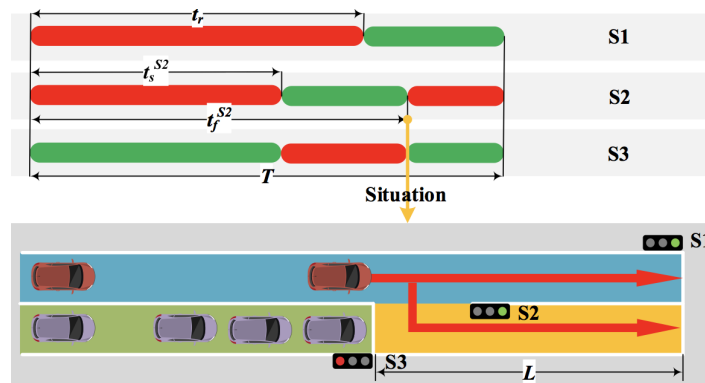


Figure 4 – Signal group timing scheme and traffic condition at the end of signal S2 green

To prevent any stopping delay after straight-through vehicles enter DSRL, the main signal S1 turns green when the straight-through vehicles reach the stop line, allowing them to pass through without stopping. Consequently, there is a constraint on the duration of signal S2 turning on the green light earlier than signal S1, as expressed in Equation 8.

$$t_r - t_s^{S2} \leq L/v_f \tag{8}$$

Once signal S1 turns green, the queue of vehicles in the STL starts to dissipate. According to the traffic wave theory, the dissipation speed of queuing vehicles in the STL can be determined using the equation  $v_w^L = \frac{Q-0}{Q/v_f - k_j}$ , and the time required for the queue of vehicles in the STL to dissipate over a distance  $L$  is given by  $t_d^L = \frac{L}{v_w^L}$ . When the queue of vehicles in STL dissipates  $L$ , as shown in Figure 4, there are two paths for straight-through vehicles to pass. To minimise the duration of right-turn vehicles coming to a stop, signal S2 terminates its green phase at this point. The duration  $t_f^{S2}$  can be determined using Equation 9.

$$t_f^{S2} = t_r + t_d^L = t_r + \frac{L}{v_w^L} = t_r + \frac{L \cdot (Q - v_f \cdot k_j) \cdot 3.6}{v_f \cdot Q} \tag{9}$$

In summary,  $t_s^{S2}$  and  $t_f^{S2}$  for signal S2 can be expressed by Equation 10.

$$t_r - \frac{L}{v_f} \leq t_s^{S2} \leq t_f^{S2} = t_r + \frac{L \cdot (Q - v_f \cdot k_j) \cdot 3.6}{v_f \cdot Q} \tag{10}$$

### 4.3 Solution method

The design parameters of DSRL control at T-shaped intersections can be optimised using the integer nonlinear programming model described above, with the objective function given by *Equations 5 and 6* and the constraints represented by *Equations 7–10*. Since this is a nonlinear programming problem, finding an optimal solution may be challenging. However, the analysis suggests that the feasible solution space is already highly constrained by the aforementioned constraints. Therefore, for different design requirements, the maximum number of calculations needed for optimisation can be estimated using *Equation 11*.

$$C = [\max(N_d) - \min(N_d) + 1] \cdot \left[ t_f^2 - \left( t_r - \frac{L}{v_f} \right) \right] \quad (11)$$

Thus, employing the enumeration method to solve the aforementioned DSRL design parameters optimisation model can fulfil the requirements of dynamic control.

## 5. CASE STUDY

### 5.1 Model fitting based on field data

This study selected the intersection of Yangshupu Road and Neijiang Road in the Yangpu District of Shanghai, China, as the research site. The intersection is of the T-shaped configuration and features the lane distribution type relevant to this study. Consequently, this intersection entrance was chosen as the target intersection entrance for this paper and depicted in *Figure 5a*. Design of DSRL signage and road markings for the target intersection entrance is presented in *Figure 5b*. The study investigates the traffic conditions at the specific entry of the T-shaped intersection. *Table 3* presents the weekday traffic demand.

*Table 3 – Traffic demand table for the weekday.*

Time-of-day	Total	Through	Right
00:00–01:00	331	165	166
01:00–02:00	273	163	110
02:00–03:00	228	136	92
03:00–04:00	191	114	77
04:00–05:00	190	114	76
05:00–06:00	386	193	193
06:00–07:00	678	406	272
07:00–08:00	1134	680	454
08:00–09:00	1562	937	625
09:00–10:00	1014	507	507
10:00–11:00	785	392	393
11:00–12:00	901	450	451
12:00–13:00	841	504	337
13:00–14:00	687	343	344
14:00–15:00	595	357	238
15:00–16:00	705	493	212
16:00–17:00	906	634	272
17:00–18:00	1385	831	554
18:00–19:00	136	518	518
19:00–20:00	784	392	392
20:00–21:00	569	284	285
21:00–22:00	445	267	178
22:00–23:00	404	202	202
23:00–24:00	381	266	115



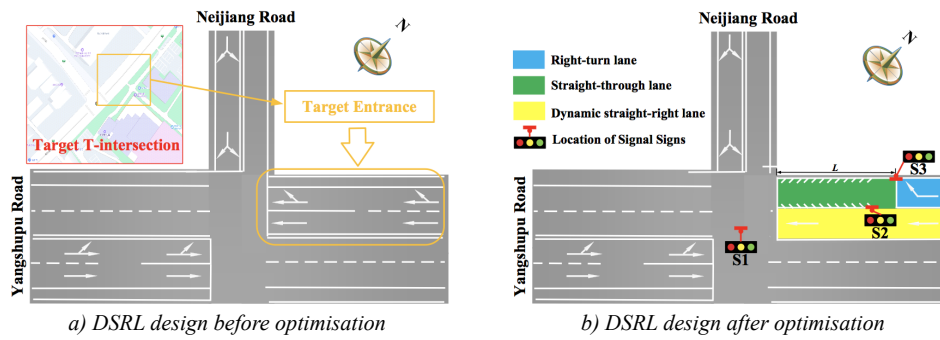


Figure 5 – Intersection of Yangshupu Road and Neijiang Road

The entrance of this T-shaped intersection consists of an STL and a straight-right lane, with a signal cycle time of 130 s and a red light duration of 75 s. The surveyed vehicles experienced an average delay of 36.16 s/veh between 8 a.m. and 9 a.m. A CA model is constructed using the *matlab2016b* software, and the traffic conditions at the entrance of the specified intersection are simulated for a duration of 3600 s. *Figure 6* illustrates the average delay variation of the simulated vehicles in the specified area.

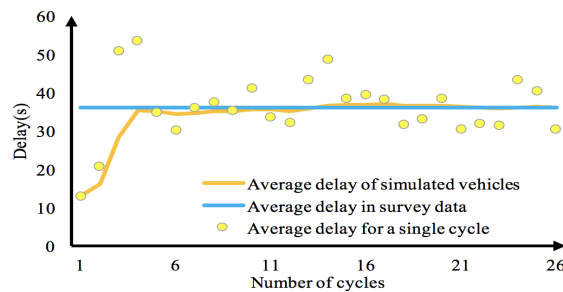


Figure 6 – Comparison graph of survey data and simulation data

With an increasing number of operating cycles, the average delay of the simulated vehicles stabilises and approaches the average vehicle delay obtained from the survey. The difference between the delays obtained from the survey and those obtained from the simulation is less than 10%, which falls within the acceptable range. Thus, this paper will proceed with the research using the constructed CA model.

### 5.2 Optimal parameters during the short-time traffic condition

According to *Table 2*, it is evident that the traffic flow reaches its peak between 8 a.m. and 9 a.m. on the specified weekday, and the optimal design parameters for DSRL control during this time period are analysed. The minimum lane-parking capacity of DSRL is  $\min(N_d)$  that set to 3 vehicles, the maximum lane-parking capacity is  $\max(N_d)$  that set to 12 vehicles, and the road jamming density of  $k_j$  is 125 veh/km. The enumeration method is utilised to identify the optimal parameters for the design of DSRL control, resulting in a total of 155 calculations, as illustrated in *Figure 7*. With a DSRL of lane-parking capacity of 9 vehicles and the green

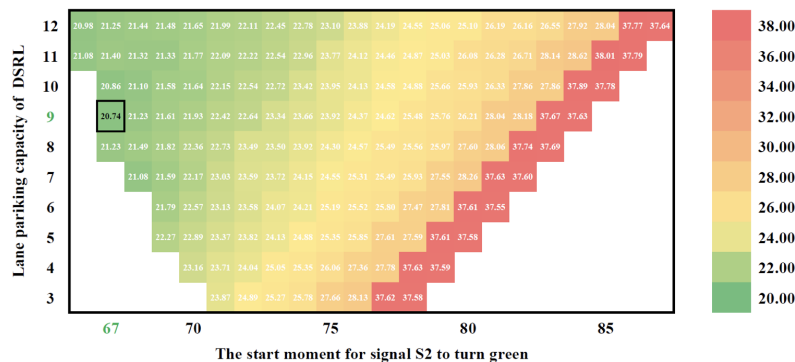
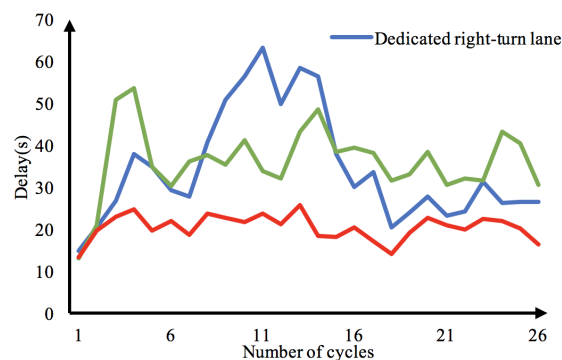


Figure 7 – Data graph for enumeration method

light of signal S2 turning on at  $t_s^{S2}=67$  s in the cycle, the average delay of simulated vehicles reaches a minimum value of 20.7 s. The DSRL control design reduces the average vehicle delay by 42% compared to the pre-optimisation average vehicle delay of 36.16 s/veh.

With the DSRL of lane-parking capacity set, the average delay of simulated vehicles generally exhibits an increasing trend as the timing of signal S2 turning green gets delayed. This is attributed to the high traffic flow at the intersection entrance, which prevents signal S2 from reaching its earliest start time when the queue length of straight-through vehicles reaches  $L$ . The straight-through vehicles are unable to enter the DSRL. In such cases, an earlier occurrence of the green light for signal S2 corresponds to an earlier entry of straight-through vehicles into the DSRL. Consequently, this leads to an earlier dissipation of queued vehicles on the STL, resulting in a smaller average delay for the simulated vehicles.

To verify the feasibility of the optimisation model calculation results, the traffic conditions during the morning peak hour from 8 a.m. to 9 a.m. were chosen. *Figure 8* compares the average vehicle delays of these two designs with that of the DSRL design.



*Figure 8* – Average vehicle delays in a single cycle for different designs

Due to the random nature of vehicle arrivals, it results in different arrivals of straight-through vehicles and right-turn vehicles during the cycle. As a result, there is a partial cycle where the average vehicle delay for the design of dedicated right-turn lane control is the largest. The design with dedicated right-turn lane control results in long queue lengths for straight-through traffic and right-turn lanes in a wasted situation, which results in wasted intersection space. When the static straight-right lane is designed to have the greatest average vehicle delay, this is because the straight-through traffic is blocking the right-turn traffic, which causes a waste of time at the intersection. Using the design of DSRL control, these two problems are solved, and it can also be seen from the simulation data that the average vehicle delay for the design of DSRL control is minimal in different cycles.

### 5.3 Optimal parameters during the whole day traffic condition

When traffic volumes vary, the minimum average vehicle delay changes differently at each lane-parking capacity as the DSRL of lane-parking capacity grows, as shown in *Figure 9*.

Minimum average vehicle delay was achieved with traffic volumes of 400 veh/h and 600 veh/h at the minimum DSRL of lane-parking capacity. This can be attributed to the low traffic volume and the limited demand for the DSRL from vehicles. At a traffic flow of 1800 veh/h, the minimum average vehicle delay is achieved when the DSRL of lane-parking capacity is maximised. This is due to the higher volume of traffic and increased vehicle demand for the DSRL, increasing the lane-parking capacity of the DSRL reduces the average vehicle delay. For other traffic flows, there exists an optimal DSRL of lane-parking capacity between the maximum and minimum values, which minimises the average vehicle delay. If the DSRL of lane-parking capacity fails to meet the vehicle demand, increasing the lane-parking capacity can reduce the average vehicle delay. When the DSRL of lane-parking capacity matches the vehicle demand, further increasing the lane-parking capacity becomes wasteful and leads to an increase in average vehicle delay.

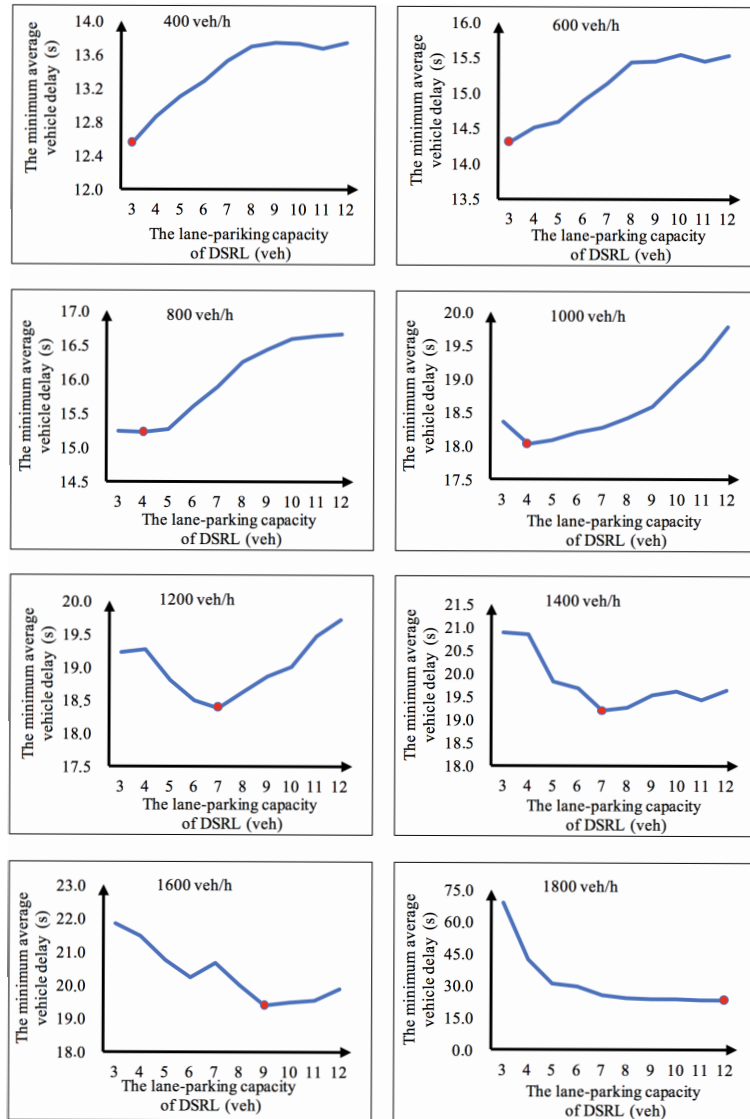


Figure 9 – Trend in minimum average vehicle delay.

To determine the optimal DSRL of lane-parking capacity for the target T-shaped intersection that caters to varying traffic volumes throughout the day, the minimum total vehicle delays are compared for different DSRL capacities during weekdays. Figure 10 illustrates that the optimal DSRL of lane-parking capacity for the selected T-shaped intersection in this study is 5 vehicles.

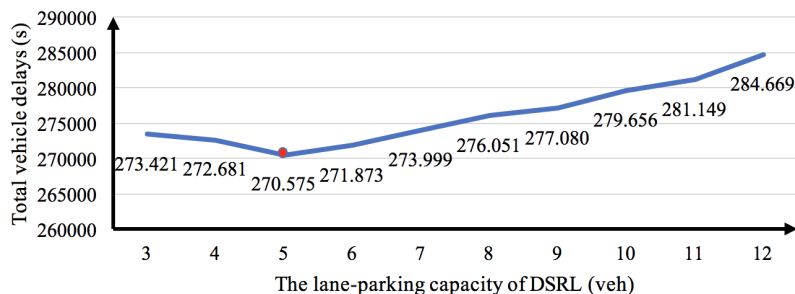


Figure 10 – Total vehicle delays for different lane-parking capacity of DSRL of weekday traffic

In the search for the optimal DSRL of lane-parking capacity, such a phenomenon was found. When the lane-parking capacity of the DSRL is determined, the signal S2 turns on the green time at different traffic volumes in order to obtain the minimum average vehicle delay. The variation of the signal S2's green time

at different traffic volumes is depicted in *Figure 11* for a DSRL of lane-parking capacity of 8 vehicles. Once the DSRL of lane-parking capacity is determined, the length of the DSRL is fixed as well. The earliest moment when signal S2 is allowed to turn on the green light and the moment when the green light goes off is influenced by the DSRL length, so both are deterministic values. At a traffic flow of 400 veh/h, the signal S2 does not need to activate the green light to achieve optimal results. When the traffic flow is 600 veh/h, 800 veh/h, 1000 veh/h and 1200 veh/h, the signal S2 needs to be on for a certain period of green time to get the best results. However, the duration of the green light is not necessarily the maximum duration for which signal S2 can remain green. Signal S2 needs to remain on for the longest duration to achieve optimal results when the traffic volume is 1400 veh/h, 1600 veh/h and 1800 veh/h.

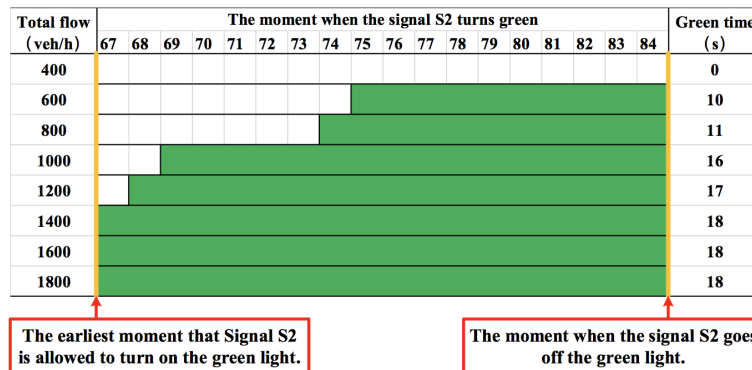


Figure 11 – The variation of the signal S2 on green time

The T-shaped intersection selected in this study has an optimal DSRL of the lane-parking capacity of 5 vehicles and the signal S2 turns on green at different times of the weekday as shown in *Figure 12*.

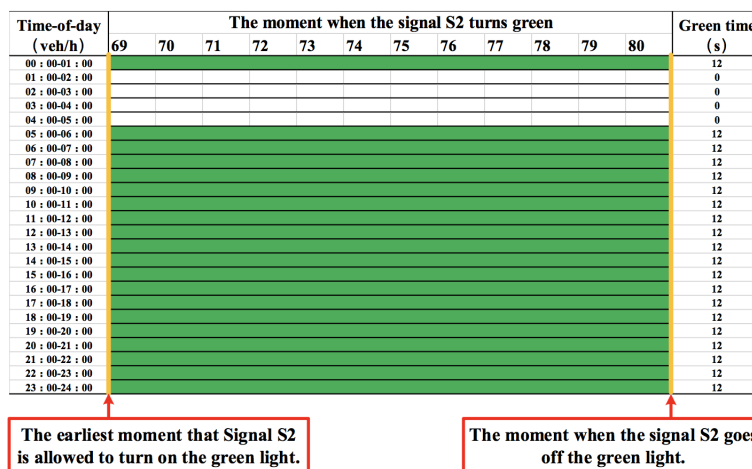


Figure 12 – The variation of the signal S2 on green time on the weekday

Between 1 a.m. and 5 a.m., the green light for Signal S2 remains off. In all other time periods, Signal S2 activates the green light with a maximum duration of 12 s. This is because the T-shaped intersection has less traffic at night, and the signal S2 is on the green which increases the average delay of vehicles. During other time periods, the vehicle demand for the DSRL exceeds its lane-parking capacity, necessitating the longest possible duration for the green light.

### 6. SENSITIVITY ANALYSES

To further investigate the performance of the proposed DSRL design, extensive sensitivity analyses are performed under various geometric and traffic conditions. The input parameters are as follows. The total flow rate at the entrance is 1600 veh/h and the cycle time of the signal set is 130 s. Five scenarios of the straight-through ratio are considered: 0.3, 0.4, 0.5, 0.6 and 0.7. The green time of S1 varies from 45 s to 65 s.

The performance of the DSRL design is compared with the dedicated right-turn lane (DRTL) design and static straight-right lane (SSRL) design. The evaluated parameters include the average vehicle delay and the optimisation rate of the comparison. The evaluation results are illustrated in *Figure 13*. It consists of 10 sub-figures. Each evaluation parameter has 5 vertically arranged subgraphs. The straight-through ratio increases from bottom to top. In each subfigure, the horizontal axes represent the green time of S1.

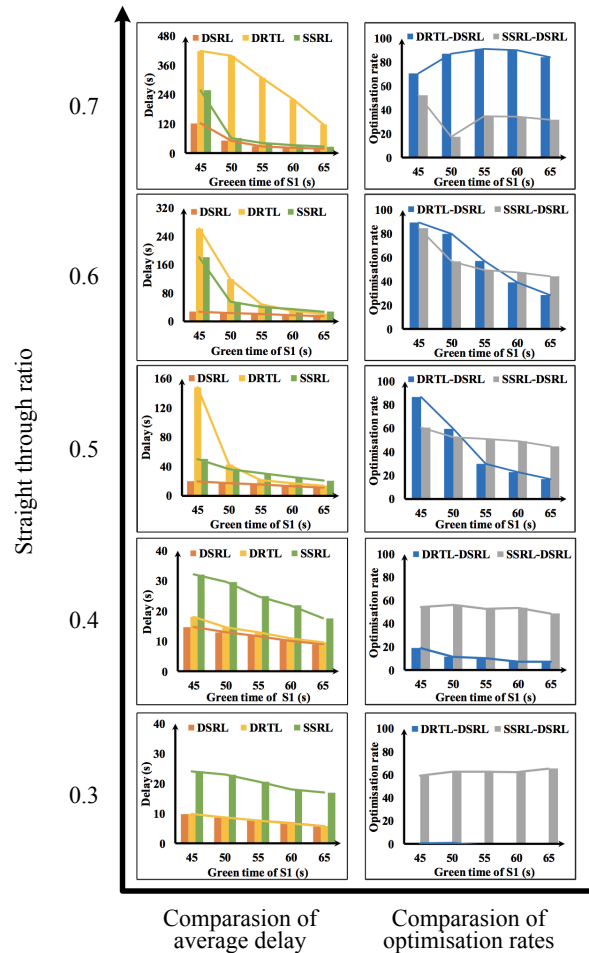


Figure 13 – Performance of DSRL design with different conditions

Overall, the average vehicle delay for DSRL is the smallest, which indicates that the DSRL design outperforms the DRTL design and SSRL design in terms of vehicle delay. This optimisation is achieved by improving upon the traditional DRTL and SSRL designs. In comparison to the DRTL design, the DSRL design incorporates additional passing lanes for straight-through vehicles. The DSRL design also mitigates the impact of straight-through vehicles on right-turn vehicles, in contrast to the SSRL design. As a result, the DSRL design enhances the efficiency of vehicle passage at the entrance.

In terms of the average vehicle delay, as the ratio of straight-through vehicles increases, the average vehicle delay increases for all three designs on the same signal S1 green time. This phenomenon occurs because straight-through vehicles are particularly impacted by signal S1 at this entrance. As the ratio of straight-through vehicles increases, more vehicles have to stop and wait due to the red light of signal S1, leading to an increase in average delay for all three designs. The figure illustrates that when the green time of signal S1 is 45 s, the average vehicle delay exceeds 130 s for all DRTL designs with a straight-through vehicle ratio of 0.5, the SSRL design with a straight-through vehicle ratio of 0.6, and the DSRL design with a straight-through vehicle ratio of 0.7. The fact that the cycle time of the signal set is 130 s suggests the formation of large-scale multiple queues by vehicles. The DSRL design can accommodate a higher proportion of straight-through vehicles compared to the other two conventional designs. This is achieved by expediting

the departure of queued straight-through vehicles using the RTL. While this may have an impact on right-turn vehicles, the reduction in delay for straight-through vehicles outweighs the increase in delay for right-turn vehicles, resulting in a decrease in the total delay for vehicles at the entrance. Although extending the green time of signal S1 can solve the phenomenon of massive multiple queues of vehicles, this measure will have an impact on the other entrances of the intersection. Therefore, the DSRL design is a good choice in order to reduce the average delay of vehicles while reducing the impact on other entrances of the intersection.

From the perspective of the optimisation rate of the comparison, as the proportion of straight traffic increases, the optimisation effect of signal intersections originally designed with DRTL is improved with the DSRL design. This is due to the increased passing pressure in the STL resulting from the higher proportion of straight-through vehicles, coupled with a decrease in right-turn vehicles and a reduced utilisation rate of the RTL. As a result, an impractical allocation of space resources at the entrance occurs, whereas the DSRL design enables dynamic allocation of resources at the entrance. The issue becomes more pronounced in the case of the DRTL design as the proportion of straight-through vehicles increases, whereas the DSRL design effectively mitigates this problem. Based on the data in the figure, it can be observed that the delay of the DSRL design is comparable to that of the DRTL design when the proportion of straight-through traffic is 0.3. This is because, according to the parameter design, it is optimal to restrict straight-through vehicles from using the DSRL, resulting in the DSRL design being equivalent to the DRTL design, thereby leading to similar delays for both designs. However, at a straight-through vehicle ratio of 0.7 and a green time of 55s for signal S1, the DSRL design achieves the highest delay reduction rate of 91% compared to the DRTL design. In contrast to the SSRL design, the primary purpose of the DSRL design is to mitigate the impact of straight-through vehicles on right-turn vehicles by dynamically controlling the RTL. This design approach aims to reduce delays for right-turn vehicles while enhancing the traffic capacity for straight-through vehicles. Based on the data, it can be concluded that the DSRL design achieves a minimum optimisation rate of 17% when the straight-through vehicle ratio is 0.7 and the green time of signal S1 is 50s. However, the DSRL design achieves the highest optimisation rate of 84% when the straight-through vehicle ratio is 0.6 and the green time of signal S1 is 45s. This is because, under the SSRL design, the intersection experiences extensive queuing of vehicles, whereas the DSRL design avoids such a phenomenon on a large scale, leading to a more pronounced optimisation effect. In conclusion, the DSRL design demonstrates superior optimisation compared to the other two conventional designs for the chosen straight-through vehicle ratio and signal S1 green time, achieving maximum optimisation rates of 91% and 84%, respectively. Consequently, implementing the DSRL design effectively enhances intersection traffic conditions.

## 7. CONCLUSION

In this paper, a design of alternative DSRL is proposed by redistributing the space-time resources at the entrance of T-shaped intersections. The data of vehicles at the entrance of T-shaped intersections are obtained by constructing a CA simulation model containing DSRL. Based on the vehicle data, the optimal design parameters for DSRL control are obtained based on the constructed optimisation model. A case study and extensive numerical analysis are conducted to evaluate the performance of the proposed design. Comparisons are made between the proposed DSRL design and the other two conventional designs, namely the DRTL design and SSRL design, under different geometric and traffic demand pattern cases. The following conclusions can be drawn.

- 1) The constructed CA model associated with the DSRL design is suitable for this study, exhibiting an error of less than 10% when compared to the actual data. Additionally, the developed optimisation model accurately determines the optimal design parameters for DSRL throughout the day, considering factors such as DSRL of lane-parking capacity and the timing of signal S2 turning green.
- 2) The DSRL design efficiently decreases the average vehicle delay by readjusting the temporal resources at T-shaped intersection entrances. In comparison to the DRTL design, the DSRL design provides additional lanes for straight-through vehicles, while compared to the SSRL design, it mitigates the hindrance caused by straight-through vehicles to right-turning vehicles.

3) The DSRL design is a good choice to improve the access conditions at the entrance while reducing the impact on other entrances of the T-shaped intersection. The maximum optimisation rate can reach 91% after switching to the DSRL design relative to the DRTL design. The maximum optimisation rate of 84% can be achieved with the DSRL design compared to the SSRL design.

To deal with the unfamiliarity of drivers, the traffic signs and markings combining the driving behaviour should be carefully studied. In addition, considering the design of dynamic straight right lane control in combination with autonomous driving technology is the direction of our future work.

## ACKNOWLEDGMENTS

This work was supported in part by the Humanities and Social Science Fund of the Ministry of Education (Grant No. 23YJCZH120), Shanghai University Students' Project for Innovation and Entrepreneurship under Grant Nos. XJ2023160, SH2023078 and 202310252023.

## REFERENCES

- [1] Liu P, et al. Capacity of U-turn movement at median openings on multilane highways. *Journal of Transportation Engineering*. 2008;134(4):147–154. DOI: 10.1061/(ASCE)0733-947X(2008)134:4(147).
- [2] Combinido JSL, Lim MT. Modeling U-turn traffic flow. *Physica A: Statistical Mechanics and its Applications*. 2010;389(17):3640–3647. DOI: 10.1016/j.physa.2010.04.009.
- [3] Zhao J, Yu J and Zhou X. Saturation flow models of exit lanes for left-turn intersections. *Journal of Transportation Engineering, Part A: Systems*. 2019;145(3). DOI: 10.1061/jtepbs.0000204.
- [4] Guo R, et al. Signal timing and geometric design at contraflow left-turn lane intersections. *International Journal of Transportation Science and Technology*. 2022;11(3):619–635. DOI: 10.1016/j.ijtst.2021.08.003.
- [5] Ding C, et al. Collaborative control of traffic signal and variable guiding lane for isolated intersection under connected and automated vehicle environment. *Computer-Aided Civil and Infrastructure Engineering*. 2021;37(15):2052–2069. DOI: 10.1111/mice.12780.
- [6] Fang Z, et al. Multivariate analysis of traffic flow using copula-based model at an isolated road intersection. *Physica A: Statistical Mechanics and its Applications*. 2022;599(127431). DOI: 10.1016/j.physa.2022.127431.
- [7] Liang S, et al. Optimization design and evaluation analysis of dynamic straight-right lane at signalized intersection. *Journal of Highway and Transportation Research and Development (English edition)*. 2022;16(1):82–91. DOI: 10.1061/JHTRCQ.0000814.
- [8] Liang S, et al. Signalized intersection dynamic straight-right lane design and evaluation. *Physica A: Statistical Mechanics and its Applications*. 2023;128771. DOI: 10.1016/j.physa.2023.128771.
- [9] Ghanbarikarekani M, Sohrabi S, Vefghi A. Optimization of signal timing of intersections by internal metering of queue time ratio of vehicles in network scale. *Promet – Traffic&Transportation*. 2016;28(3):205–214. DOI:10.7307/ptt.v28i3.1729.
- [10] Yang Q, et al. Modeling the permissive-only left-turn queue at signals. *Physica A: Statistical Mechanics and its Applications*. 2019;525:315–325. DOI:10.1016/j.physa.2019.03.070.
- [11] Yang Q, Shi Z. The queue dynamics of protected/permissive left turns at pre-timed signalized intersections. *Physica A: Statistical Mechanics and its Applications*. 2021;562(125406). DOI: 10.1016/j.physa.2020.125406.
- [12] Yang Q, et al. Characterizing the dynamics and uncertainty of queues at signalized intersections with left-turn bay. *Physica A: Statistical Mechanics and its Applications*. 2022;599(127439). DOI: 10.1016/j.physa.2022.127439.
- [13] Yang Q, He Y. Right-turn-on-red queueing process at signalized intersections with a short right-turn lane. *Physica A: Statistical Mechanics and its Applications*. 2022;598(127395). DOI: 10.1016/j.physa.2022.127395.
- [14] Zhao J, et al. Increasing the capacity of signalized intersections with dynamic use of exit lanes for left-turn traffic. *Transportation Research Record: Journal of the Transportation Research Board*. 2013;2355(1):49–59. DOI: 10.3141/2355-06.

- [15] Xuan Y, Daganzo CF, Cassidy MJ. Increasing the capacity of signalized intersections with separate left turn phases. *Transportation Research Part B: Methodological*. 2011;45(5):769–781. DOI: 10.1016/j.trb.2011.02.009.
- [16] Chen Q, Yi J, Wu Y. Cellular automaton simulation of vehicles in the contraflow left-turn lane at signalised intersections. *IET Intelligent Transport Systems*. 2019;13(7):1164–1172. DOI: 10.1049/iet-its.2018.5451.
- [17] Liu P, et al. Estimating queue length for contraflow left-turn lane design at signalized intersections. *Journal of Transportation Engineering, Part A: Systems*. 2019;145(6). DOI: 10.1061/jtepbs.0000240.
- [18] Zhao J, Ma W. An alternative design for the intersections with limited traffic lanes and queuing space. *IEEE Transactions on Intelligent Transportation Systems*. 2021;22(3):1473–1483. DOI: 10.1109/tits.2020.2971353.
- [19] Wu J, et al. Developing an actuated signal control strategy to improve the operations of contraflow left-turn lane design at signalized intersections. *Transportation Research Part C: Emerging Technologies*. 2019;104:53–65. DOI: 10.1016/j.trc.2019.04.028.
- [20] Wu J, et al. Operational analysis of the contraflow left-turn lane design at signalized intersections in China. *Transportation Research Part C: Emerging Technologies*. 2016;69:228–241. DOI: 10.1016/j.trc.2016.06.011.
- [21] Chen X, Jia Y. Sustainable traffic management and control system for arterial with contraflow left-turn lanes. *Journal of Cleaner Production*. 2021;280(124256). DOI: 10.1016/j.jclepro.2020.124256.
- [22] Wu J, et al. Stationary condition based performance analysis of the contraflow left-turn lane design considering the influence of the upstream intersection. *Transportation Research Part C: Emerging Technologies*. 2021;122(102919). DOI: 10.1016/j.trc.2020.102919.
- [23] Wolshon B, Lambert L. Reversible lane systems: Synthesis of practice. *Journal of Transportation Engineering*. 2006;132(12):933–944. DOI: 10.1061/(ASCE)0733-947X(2006)132:12(933).
- [24] Di Z, Yang L. Reversible lane network design for maximizing the coupling measure between demand structure and network structure. *Transportation Research Part E: Logistics and Transportation Review*. 2020;141(102021). DOI: 10.1016/j.tre.2020.102021.
- [25] Zhao J, et al. Operational efficiency evaluation of intersections with dynamic lane assignment using field data. *Journal of Advanced Transportation*. 2017;2017:1–13. DOI: 10.1155/2017/2130385.
- [26] Karoonsoontawong A, Lin DY. Time-varying lane-based capacity reversibility for traffic management. *Computer-Aided Civil and Infrastructure Engineering*. 2011;26(8):632–646. DOI: 10.1111/j.1467-8667.2011.00722.x.
- [27] Frejo JRD, et al. Macroscopic modeling and control of reversible lanes on freeways. *IEEE Transactions on Intelligent Transportation Systems*. 2016;17(4):948–959. DOI: 10.1109/tits.2015.2493127.
- [28] Zhang L, Wu G. Dynamic lane grouping at isolated intersections: Problem formulation and performance analysis. *Transportation Research Record: Journal of the Transportation Research Board*. 2012;2311(1):152–166. DOI: 10.3141/2311-15.
- [29] Zhao J, Liu Y, Yang X. Operation of signalized diamond interchanges with frontage roads using dynamic reversible lane control. *Transportation Research Part C: Emerging Technologies*. 2015;51:196–209. DOI: 10.1016/j.trc.2014.11.010.
- [30] Xie C, Turnquist MA. Lane-based evacuation network optimization: An integrated Lagrangian relaxation and tabu search approach. *Transportation Research Part C: Emerging Technologies*. 2011;19(1):40–63. DOI: 10.1016/j.trc.2010.03.007.
- [31] Kotagi PB, Asaithambi G. Microsimulation approach for evaluation of reversible lane operation on urban undivided roads in mixed traffic. *Transportmetrica A: Transport Science*. 2019;15(2):1613–1636. DOI: 10.1080/23249935.2019.1632387.
- [32] Hao Y, et al. Increasing capacity of intersections with transit priority. *Promet – Traffic&Transportation*. 2016;28(6):627–637. DOI: 10.7307/ptt.v28i6.1999.
- [33] Huang J, et al. Effect of pre-signals in a Manhattan-like urban traffic network. *Physica A: Statistical Mechanics and its Applications*. 2018;503:71–85. DOI: 10.1016/j.physa.2018.02.170.
- [34] Gu W, et al. An integrated intersection design for promoting bus and car traffic. *Transportation Research Part C: Emerging Technologies*. 2021;128(103211). DOI: 10.1016/j.trc.2021.103211.
- [35] Liu M, et al. An adaptive timing mechanism for urban traffic pre-signal based on hybrid exploration strategy to improve double deep Q network. *Complex & Intelligent Systems*. 2022;9(2):2129–2145. DOI: 10.1007/s40747-022-00903-6.



- [36] Nagel K, Schreckenberg M. A cellular automaton model for freeway traffic. *Journal de Physique I*. 1992;2(12):2221–2229. DOI: 10.1051/jp1:1992277.
- [37] Rickert M, et al. Two lane traffic simulations using cellular automata. *Physica A: Statistical Mechanics and its Applications*. 1996;231(4):534–550. DOI: 10.1016/0378-4371(95)00442-4.
- [38] El Dessouki WM, Fathi Y, Roupail N. Meta-optimization using cellular automata with application to the combined trip distribution and assignment system optimal problem. *Computer-Aided Civil and Infrastructure Engineering*. 2002;16(6):384–398. DOI: 10.1111/0885-9507.00241.
- [39] Li XG, et al. A realistic two-lane cellular automata traffic model considering aggressive lane-changing behavior of fast vehicle. *Physica A: Statistical Mechanics and its Applications*. 2006;367:479–486. DOI: 10.1016/j.physa.2005.11.016.
- [40] Wang J, et al. A multi-agent based cellular automata model for intersection traffic control simulation. *Physica A: Statistical Mechanics and its Applications*. 2021;584(126356). DOI: 10.1016/j.physa.2021.126356.
- [41] Liu S, Kong D, Sun L. Cellular automata model for traffic flow with optimised stochastic noise parameter. *Promet – Traffic&Transportation*. 2022;34(4):567–580. DOI: 10.7307/ptt.v34i4.4049.

韩印，宁搏，梁士栋

一种可替代的T型交叉口动态直右车道控制的优化设计

摘要：

动态直右车道控制设计被作为一种非常规的信号交叉口控制方法被提出，该设计运用右转车道的资源来提高直行交通的通行效率，同时尽量减少对右转车辆的影响。本文针对T型信号交叉口提出了一种可替换的动态直右车道控制优化设计，该设计通过对进口处的时空资源进行重新设计，可保障车辆换道行为的安全，同时也可降低T型交叉口使用该设计的门槛。运用本文构建的适用于动态直右车道控制设计的元胞自动机模型，可获取动态直右车道控制的优化设计模型所需数据，并通过一个实际案例，获取动态直右车道控制的最优设计参数。本文在不同的几何和交通需求情况下，将提出的 DSRL 控制设计与两种传统控制设计（即专用右转车道控制设计和静态直右车道控制设计）进行了比较。研究表明，当 T 形交叉口选用专用右转车道控制设计时，采用 DSRL 控制设计的最大延迟优化率可达到 91%，当 T 形交叉口选用静态直右车道控制设计时，采用 DSRL 控制设计的最大延迟优化率可达到 84%。

关键词：

T形交叉口，动态控制，元胞自动机，交通优化